



Virginia Commonwealth University
VCU Scholars Compass

Electrical and Computer Engineering Publications

Dept. of Electrical and Computer Engineering

2003

Current mapping of GaN films by conductive atomic force microscopy

A. A. Pomarico

Virginia Commonwealth University

D. Huang

Virginia Commonwealth University

J. Dickinson

Virginia Commonwealth University

See next page for additional authors

Follow this and additional works at: http://scholarscompass.vcu.edu/egre_pubs

 Part of the [Electrical and Computer Engineering Commons](#)

Pomarico, A.A., Huang, D., Dickinson, J., et al. Current mapping of GaN films by conductive atomic force microscopy. *Applied Physics Letters*, 82, 1890 (2003). Copyright © 2003 AIP Publishing LLC.

Downloaded from

http://scholarscompass.vcu.edu/egre_pubs/67

This Article is brought to you for free and open access by the Dept. of Electrical and Computer Engineering at VCU Scholars Compass. It has been accepted for inclusion in Electrical and Computer Engineering Publications by an authorized administrator of VCU Scholars Compass. For more information, please contact libcompass@vcu.edu.

Authors

A. A. Pomarico, D. Huang, J. Dickinson, A. A. Baski, R. Cingolani, Hadis Morkoç, and R. Molnar

Current mapping of GaN films by conductive atomic force microscopy

A. A. Pomarico,^{a)} D. Huang,^{b)} J. Dickinson, A. A. Baski, R. Cingolani,^{a)} and H. Morkoç^{c)}
*Virginia Commonwealth University, Department of Electrical Engineering and Physics Department,
 Richmond, Virginia 23284*

R. Molnar

Massachusetts Institute of Technology, Lincoln Laboratory, Lexington, Massachusetts 02173

(Received 9 December 2002; accepted 30 January 2003)

Conductive atomic force microscopy has been used to investigate the local conductivity in hydride vapor-phase epitaxy and molecular-beam epitaxy GaN films, focusing on the effect of off-axis facet planes. We investigated two different types of samples, in which the facet planes were either present on the perimeters of as-grown islands, or on the edges of etch pits created by post-growth chemical etching. The results show that crystallographic planes tilted with respect to the *c*-plane growth direction show a significantly higher conductivity than surrounding areas. The *n*-type (or *p*-type) samples required a negative (or positive) sample bias for current conduction, consistent with the formation of a Schottky barrier between the metallized atomic force microscope tip and sample. The time dependence of this enhanced conductivity was different for the two types of samples, possibly indicating different conduction mechanisms. © 2003 American Institute of Physics.

[DOI: 10.1063/1.1563054]

GaN-based semiconductors have great technological potential^{1–4} in optoelectronic⁵ and high-power, high-frequency, applications. In order to take full advantage of this material system, however, it is essential to gain a deeper understanding of its properties. In particular, electrical characteristics are under study because current leakage under reverse bias in GaN-based electronic devices remains the main obstacle in their use for field-effect transistors applications.⁶ A recently developed technique for studying the local electrical properties of samples is conductive atomic force microscopy (C-AFM). By simultaneously mapping topography and current on a surface, C-AFM allows one to correlate electrical properties with surface topography. C-AFM investigations by Hsu *et al.*⁷ have shown that reverse-bias current in molecular-beam epitaxy (MBE)-grown GaN samples occurs primarily at screw dislocations, suggesting that they can act as leakage paths. Miller *et al.*⁸ also observed conductive screw or mixed dislocations in MBE-grown GaN/AlGaIn heterostructures under reverse bias, although dislocations with a screw component that did not conduct current were also apparent in their study. In this work, we use C-AFM to map out local current variations on etched and as-grown GaN films, focusing on the effect of off-axis facet planes on current conduction.

These experiments were performed on GaN samples grown on *c*-plane sapphire either by MBE or hydride vapor-phase epitaxy (HVPE). The results presented here include data for etched *n*-type or *p*-type HVPE samples, and for an as-grown MBE sample. The HVPE samples included an *n*-type, Si-doped GaN film ($n \sim 2 \times 10^{18} \text{ cm}^{-3}$, 9.4- μm

thick), and a *p*-type, Zn-doped film (17.3- μm thick). The Si-doped sample was etched with molten KOH for 6 min at 210 °C, and the Zn-doped sample was etched with phosphoric acid H₃PO₄ at 160 °C for 2 min. The etching process preferentially removed material at dislocation defects, producing etch pits with off-axis planes along their perimeters. The as-grown MBE sample in this study was of interest because hexagonal islands with off-axis planes were present. This 1.2- μm -thick GaN film was grown at ~ 800 °C on an AlN buffer layer, where a series of ten alternating layers of AlN and GaN were inserted below the GaN film to minimize defect propagation. This sample is unintentionally *n*-type doped ($n \sim 1.1 \times 10^{17} \text{ cm}^{-3}$).

For the C-AFM measurements, a Dimension 3100 atomic force microscope (AFM) was operated in contact mode with an electrically conductive probe. A low-noise amplifier then detected localized current between the AFM tip and sample when a dc bias was applied. The range of detectable currents was 10 pA to 10 nA for the C-AFM module amplifier. Figure 1 shows schematically the experimental arrangement and equivalent circuit. Both metal-coated and highly doped, diamond-coated tips were used, where the tip-to-sample contact behaved as a microscopic Schottky contact. During C-AFM operation, a feedback loop maintained a constant cantilever deflection (or force), and the amplifier measured any tip-to-sample current. Simultaneous images of the sample topography and current were then obtained, allowing one to correlate localized current with sample features.

The AFM topography and C-AFM current images of the two etched HVPE samples are shown in Figs. 2 and 3. The surface morphologies of these samples show the expected hexagonal-shaped pits produced by etching of defect sites on *c*-plane GaN.^{9–13} The etch pit densities of the two samples are similar: $\sim 6 \times 10^8 \text{ cm}^{-2}$ for the *n*-type, Si-doped film, and $\sim 3 \times 10^8 \text{ cm}^{-2}$ for the *p*-type, Zn-doped film. The hex-

^{a)}Also with: NNL National Nanotechnology Laboratory of INFN, Università di Lecce, Via per Arnesano, I-73100 Lecce, Italy.

^{b)}Also with: Physics Department, Fudan University, Shanghai 200433, China.

^{c)}Author to whom correspondence should be addressed; electronic mail: hmorkoc@vcu.edu

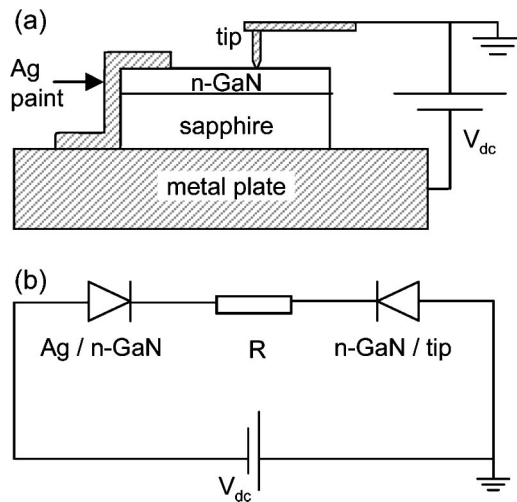


FIG. 1. Schematic diagrams showing (a) experimental setup and (b) equivalent circuit for *n*-type GaN at negative bias with respect to tip. “*R*” represents the bulk resistance of the GaN film.

agonal etch pits are slightly larger on the *n*-type sample (50–450 nm diam., 20–200 nm depth) versus the *p*-type one (130–330 nm and 10–140 nm). In both cases, however, the internal walls of the etch pits form an angle of 45° to 55° with the *c*-plane.

With regard to the C-AFM data, current was only detected for the etched HVPE samples under forward-bias conditions, that is, negative sample-to-tip voltage for the *n*-type sample and positive voltage for the *p*-type one. For similar voltages, however, the *n*-type sample resulted in higher current values than the higher resistivity *p*-type sample. In the case of the *n*-type sample, a majority of the sample surface was conducting at higher bias voltages (–4 to –12 V), and only localized regions showed a detectable current signal at smaller voltages (–1 to –4 V). The simultaneous AFM and C-AFM current images for this sample are shown in Fig. 2 and were taken at –1 V bias voltage. A comparison of the images indicates that the only measurable current under

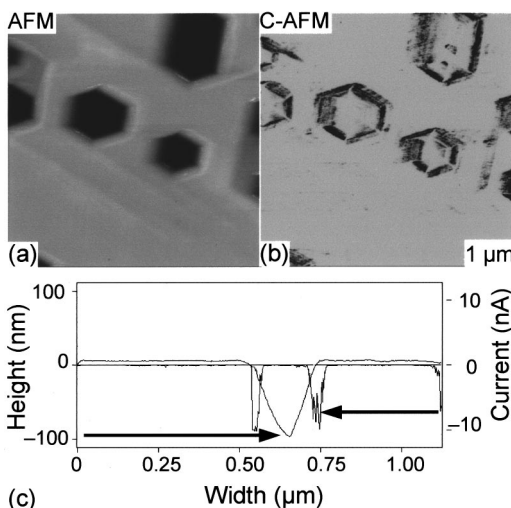


FIG. 2. (a) AFM surface morphology and (b) C-AFM current images of an etched, *n*-type, Si-doped HVPE GaN sample. The sample-to-tip voltage is –1.0 V. The vertical scales are (a) 60 nm and (b) 10 nA, and both image sizes are 1 μm × 1 μm, as indicated. (c) Dual cross section of one of the etch pits with the topography and current signals superimposed. An increased current signal is observed on the edges of the pit.

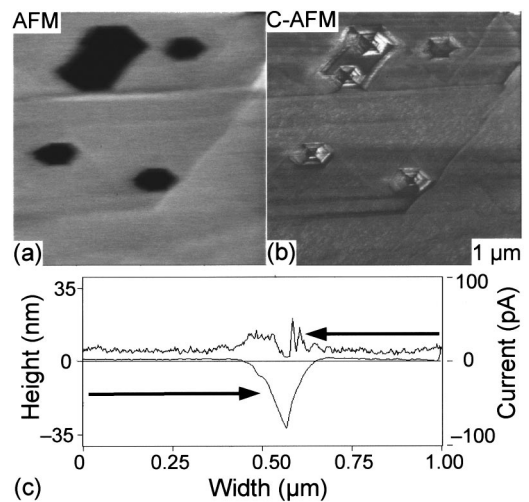


FIG. 3. (a) Surface morphology and (b) current images of an etched, Zn-doped HVPE sample, with a sample to tip voltage of +3 V. The vertical scales are (a) 15 nm and (b) 200 pA. (c) Dual cross section of one of the etch pits with the topography and current signals superimposed.

these bias conditions occurs at the edges of the etch pits. A dual cross-section [Fig. 2(c)] of one of these pits shows a maximum current value of 10 nA, corresponding to an effective tip–sample resistance of $\sim 10^8 \Omega$. The *p*-type sample shown in Fig. 3 also indicates enhanced current at the edges of the etch pits. In this case, the current is only ~ 20 pA for +3 V bias, yielding an effective resistance of $\sim 10^{11} \Omega$. The highest measured currents on this sample were ~ 120 pA at +6 V, a value more than three orders of magnitude smaller than that seen for the *n*-type sample. Similar C-AFM results showing enhanced current on the sidewalls of etch pits have also been obtained for etched, MBE-grown GaN samples.

In addition to the etched samples, an as-grown MBE sample having hexagonal islands was examined [see Fig. 4(a)]. The lateral facets or walls of these columns are oriented 20° to 40° from the *c*-plane. The islands themselves are 300 to 420 nm in diameter, 20 to 90 nm tall, and have a density of $2 \times 10^6 \text{ cm}^{-2}$. As expected, this *n*-type sample only shows measurable current in the forward bias condition,

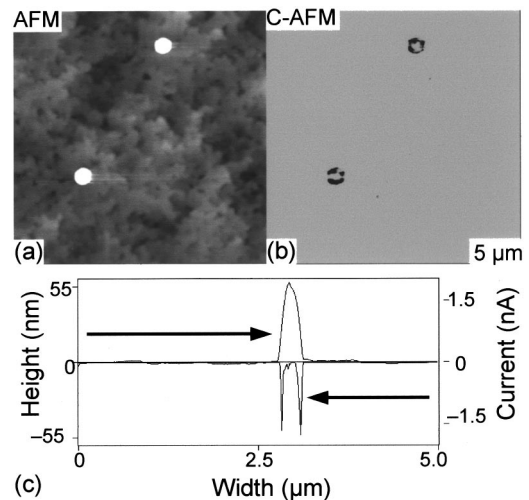


FIG. 4. (a) Surface morphology and (b) current images of an as-grown MBE GaN sample, with a sample to tip voltage of –3 V. The vertical scales are (a) 20 nm and (b) 1 nA. (c) Dual cross section of one of the hexagonal islands, which indicates increased current on the edges of the island.

that is, under negative sample voltage. Similar to the C-AFM results for etch pits, current is detected primarily along the edges of prominent features, or islands in this case. The cross section in Fig. 4(c) indicates a current along the island edges of ~ 1.5 nA for -3 V bias. Most islands were observed to be conducting for a bias voltage from -1 to -4 V. It should be noted that C-AFM images for this sample did exhibit a time dependence, unlike for the etched samples. After multiple scans in the same region, the current gradually decreased to zero in a matter of minutes. For example, a $2 \times 2 \mu\text{m}^2$ image scanned at 0.5 Hz/s showed no current signal after two to three scans.

Our C-AFM results from both the etched and as-grown samples show enhanced current conduction at the edges of pits or islands. This indicates that the off-axis planes situated at such locations are more electrically active than *c*-plane GaN. It has been reported that the N-face of *c*-plane GaN has a lower Schottky barrier height than Ga-face.^{14,15} If the same were true for the *a*, *r*, and *m* planes of GaN, then increased current conduction could be expected on those surfaces. The enhanced conduction for the etch pits could also be related to their origin near defect sites on the sample. Screw dislocations were found to be the dominant defect in the case of the Si-doped HVPE sample. Prior C-AFM studies have shown that such dislocations may provide channels for large and stable current.⁷ In contrast, the increased conduction of the island sidewalls on the as-grown sample is most likely not associated with dislocations. This could explain the reduced current seen for these off-axis planes after multiple scans, because bulk charge is not available via dislocations to replenish the surface charge. The experimental results also showed a substantial current difference between the etched *n*-type and Zn-doped samples. This may be primarily due to higher bulk resistivity of the Zn-doped sample as compared to the *n*-type one. However, differences in such properties as the surface potential barrier height, adsorbed impurities, and the surface charges may also affect the current.

In conclusion, we have observed enhanced conductivity for the off-axis facet planes present on as-grown and etched GaN films. On more highly doped *n*-type samples, currents

on the order of nanoamperes were measured along the edges of etch pits for negative sample bias voltages of a few volts. No detectable current was found for positive bias voltages, consistent with the formation of a Schottky contact between the AFM tip and sample. The conduction behavior observed for the sidewalls of post-growth etch pits versus as-grown islands was qualitatively different. The off-axis planes on the island edges lost their enhanced conductivity after multiple scans, indicating that limited bulk charge was available. This behavior was in contrast to the stable currents found along the edges of the etch pits. Possible mechanisms for the enhanced current conduction observed on off-axis planes could be related to modified Schottky barrier heights or the presence of dislocations.

This research was funded by grants from NSF (Dr. L. Hess and Dr. U. Varshney), AFOSR (Dr. G. L. Witt), and ONR (Dr. C. E. C. Wood and Dr. Y. S. Park).

¹H. Morkoç, *Nitride Semiconductors and Devices* (Springer, Heidelberg, 1999).

²S. T. Strite and H. Morkoç, *J. Vac. Sci. Technol. B* **10**, 1237 (1992).

³O. Ambacher, *J. Phys. D* **31**, 2653 (1998).

⁴S. J. Pearton, J. C. Zolper, R. J. Shu, and F. Ren, *J. Appl. Phys.* **86**, 1 (1999).

⁵S. Nakamura and G. Fasol, *The Blue Laser Diode* (Springer, Berlin, 1997).

⁶M. E. Levinshtein, S. L. Rumyantsev, R. Gaska, J. W. Wang, and M. S. Shur, *Appl. Phys. Lett.* **73**, 1089 (1998).

⁷J. W. P. Hsu, M. J. Manfra, D. V. Lang, S. Richter, S. N. G. Chu, A. M. Sergent, R. N. Kleiman, L. N. Pfeiffer, and R. J. Molnar, *Appl. Phys. Lett.* **78**, 1685 (2001).

⁸E. J. Miller, D. M. Schaadt, E. T. Yu, C. Poblentz, C. Elsass, and J. S. Speck, *J. Appl. Phys.* **91**, 9821 (2002).

⁹T. Kozawa, T. Kaxhi, T. Ohwaki, Y. Taga, N. Koide, and M. Koike, *J. Electrochem. Soc.* **143**, L17 (1996).

¹⁰S. K. Hong, B. J. Kim, H. S. Park, Y. Park, S. Y. Yoon, and T. I. Kim, *J. Cryst. Growth* **191**, 275 (1998).

¹¹K. Shiojima, *J. Vac. Sci. Technol. B* **18**, 37 (2000).

¹²T. Hino, S. Tomiya, T. Miyajima, K. Yanashima, S. Hashimoto, and M. Ikeda, *Appl. Phys. Lett.* **76**, 3421 (2000).

¹³D. A. Stocker, E. F. Schubert, and J. M. Redwing, *Appl. Phys. Lett.* **73**, 2654 (1998).

¹⁴Z.-Q. Fang, D. C. Look, P. Visconti, D.-F. Wang, C.-Z. Lu, F. Yun, H. Morkoç, S. S. Park, and K. Y. Lee, *Appl. Phys. Lett.* **78**, 2178 (2001).

¹⁵U. Karrer, O. Ambacher, and M. Stutzmann, *Appl. Phys. Lett.* **77**, 2012 (2000).